



Pt-impregnated catalysts on powdery SiC and other commercial supports for the combustion of hydrogen under oxidant conditions

G.M. Arzac*, O. Montes, A. Fernández*

Instituto de Ciencia de Materiales de Sevilla (CSIC-Univ. Sevilla), Avda. Américo Vespucio 49, 41092, Sevilla, Spain



ARTICLE INFO

Article history:

Received 13 May 2016

Received in revised form 2 August 2016

Accepted 16 August 2016

Available online 17 August 2016

Keywords:

Hydrogen

Catalytic combustion

Pt-impregnated catalysts

Powdery SiC

ABSTRACT

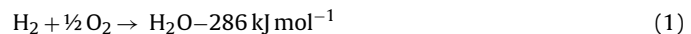
We report the study of the catalytic hydrogen combustion over Pt-impregnated powdery silicon carbide (SiC) using H_2PtCl_6 as precursor. The reaction was conducted in excess of oxygen. β -SiC was selected for the study because of its thermal conductivity, mechanical properties, chemical inertness and surface area. The obtained Pt particles over SiC were medium size (average particle diameter of 5 nm for 0.5 wt% Pt). The activity of the Pt-impregnated catalyst over SiC was compared to those obtained in oxidized form over TiO_2 and Al_2O_3 commercial supports (Pt particles very small in size, average particle diameter of 1 nm for 0.5 wt% Pt in both cases). The case of a SiO_2 support was also discussed. Those Pt/SiC particles were the most active because of their higher contribution of surface Pt^0 , indicating that partially oxidized surfaces have better activity than those totally oxidized in these conditions. SiC was modified with an acid treatment and thus bigger (average particle diameter of 7 nm for 0.5 wt% Pt) and more active Pt particles were obtained. Durability of the SiC and TiO_2 supported catalysts was tested upon 5 cycles and both have shown to be durable and even more active than initially. Exposure to the oxidative reaction mixture activates the catalysts and the effect is more pronounced for the completely oxidized particles. This is due to the surface oxygen chemisorption which activates catalystsí surface.

© 2016 Elsevier B.V. All rights reserved.

1. Introduction

It is now generally accepted that in a near future, the world should move towards a greener energetic paradigm. Fossil fuelsí scarcity and the environmental issues related to their extensive use make necessary to think on another energy sources and carriers. In this context, hydrogen appears as a clean energy vector with an attractive energy density (142 MJ kg⁻¹ while for liquid hydrocarbons is 47 MJ kg⁻¹) [1–3]. Once obtained through green resources, hydrogen can produce energy upon generating water as only byproduct. For the implementation of the use of hydrogen, challenges related to production, transportation, storage and combustion should be met first. The catalytic hydrogen combustion (CHC, reaction (1)) is a key reaction in the “hydrogen economy” which can be employed as a means of heat production (cookers, heaters, etc) as well as for safety purposes (elimination of undesired hydrogen) [4–17]. For heat production applications, high amounts of hydrogen rich mixtures are preferred. Regarding safety purposes, the amount of undesired hydrogen to be eliminated can range from

large amounts in the nuclear industry (in case of an accident) to the byproducts of chemical and petrochemical industries or during the operation of various electrochemical processes. Small amounts of hydrogen can be released in the exhaust of fuel cells and its accumulation may constitute a hazard. In this field, the study of CHC in lean hydrogen/air mixtures is especially relevant. For this type of application it is desirable to use catalysts which are active enough to start the reaction even at room temperature. In this sense Pt and Pd oxides are the most appropriate according to previous report [4].



Reaction (1) is also interesting from a fundamental point of view. It may contribute to develop fundamental understanding of catalytic oxidation reactions and permits to test metal catalysts in both reducing and oxidizing atmospheres (excess of hydrogen or oxygen respectively).

For practical applications, catalyst should be prepared in supported form, which improves dispersion, prevents aggregation and facilitates its use in successive cycles. Most papers report the use of metal oxides such as SiO_2 , TiO_2 , CeO_2 , SnO_2 , ZrO_2 , but only recent works report the use of SiC [7,14,17,18]. Silicon carbide (especially cubic phase, β -SiC) is a highly advantageous support because of its relatively high specific surface area, chemical inertness, thermal

* Corresponding authors.

E-mail addresses: gisela@icmse.csic.es (G.M. Arzac), [\(A. Fernández\)](mailto:asuncion@icmse.csic.es).

conductivity and mechanical properties [19–22]. The use of SiC as catalyst support is a growing field of research and was reported for reactions like *n*-butane partial oxidation, H₂S selective oxidation and methanol dehydration [23–25]. SiC was also recently studied as support for the deposition of Co nanoparticles in the study of the Fischer Tropsh (FTS) reaction [26,27]. The problem with SiC is its inert and hydrophobic surface which suffers from scarcity of reactive sites for the adsorption of the metal ions during catalyst preparation. To circumvent this, several strategies such as thermal or acid treatments can be employed [19,28].

In this paper, we have studied the CHC under excess of oxygen (lean, 1% v/v H₂/air mixture) on Pt-impregnated catalysts over powdery commercial SiC and compared with those traditionally used supports. We have prepared the Pt catalysts in their oxidized form over SiC, TiO₂, SiO₂ and Al₂O₃ powders and their activity was compared. We have also intended to modify the SiC support with an acid treatment in order to make its surface more reactive to metal ion adsorption for a better dispersion of the active phase. Some catalytic tests with pre-reduced catalysts are also included. Trends in catalytic activity and durability are discussed herein in connection to the nature of the support, surface, particle size and dispersion. Practical conclusions are also obtained regarding the use of SiC as catalyst support for this important but scarcely studied reaction.

2. Experimental section

2.1. The supports

Commercial TiO₂ (nanopowder, 21 nm particle size, Sigma Aldrich), Al₂O₃ (neutral, 50–200 μm particle size, Sigma Aldrich) and SiC (nanopowder, less than 100 nm particle size, Sigma Aldrich) were used as received. The supports were first characterized regarding surface area and zeta potential and results are supplied as Supporting information (Fig. 1S). The SiO₂ support was prepared by calcining the commercial SiC at 1000 °C 7 h under static air (4.2 °C/min ramp) [28]. Optimization of calcination conditions and characterization of the prepared SiO₂ can be also found in the Supporting information. Except for the alumina powder, the rest of the supports have comparable surface area according to BET measurements (see Fig. 1S).

SiC commercial powder was also further modified to improve its surface composition [19]. It was treated in acidic medium in order to introduce hydrophilic surface Si—O groups and thus make its surface more reactive to metal ion adsorption for a better dispersion of the active phase. Commercial SiC (300 mg) was treated with an acidic solution of H₂SO₄ (10 ml) and HNO₃ (10 ml) and 1 ml of MilliQ® water [19]. The mixture was put in an ultrasonic bath for 15 min and then heated under reflux for 1.5 h. The product was centrifuged (1000 rpm, 10 min) and washed with 20 ml of water five times. The solid was dried at 120 °C overnight.

2.2. Catalysts' preparation

Catalysts were prepared by pore volume impregnation of the support with aqueous H₂PtCl₆·6H₂O (Sigma Aldrich). When using SiC as support the aqueous H₂PtCl₆·6H₂O solution contained 10% v/v ethanol in order to increase support wettability. The Pt loading was calculated for a final amount of 1 and 0.5 wt% as will be indicated along the text (sample will be named indicating Pt load and support, see Table 1). The pH of the impregnating solution was around 0. The H₂PtCl₆ concentration in the impregnation solutions depends on the desired loading, the nature of the support and its pore volume, and in this work it is in the range of 0.026–0.06 M. After impregnation, catalysts were dried at 120 °C for 12 h and then calcined in static air at 400 °C during 4 h (3 °C/min ramp). These con-

ditions favor the formation of platinum oxides on catalysts' surface and the degree of oxidation will depend on the particle size.

2.3. Catalysts' characterization

For TEM (Transmission Electron Microscopy) studies, samples were dispersed in ethanol by ultrasound and dropped on a copper grid. Measurements were performed on a FEI Tecnai G2 F30 FEG (field emission gun) microscope, equipped with a HAADF (High Angle Annular Dark Field) detector from Fischione Instruments, and operated in STEM (scanning TEM) mode at 300 kV. The Pt particle size distributions were evaluated from the TEM micrographs. The images were processed with an image processing software (Adobe Photoshop) to identify the particles as well-defined dark contrast areas which were then analyzed with the ImageJ software.

X-ray diffraction measurements were performed using the Cu K α radiation in a Siemens D5000 diffractometer in a Bragg-Brentano configuration in the 2θ angle range of 10–90°. XPS spectra were recorded with a Leybold Heraus LH electron spectrometer using Al K α radiation with 40 eV pass energy at normal emission take off angle. The alumina and titania supported materials' spectra were calibrated with the signal of C 1s at 284.6 eV (contamination). Those SiC and SiO₂ supported materials' spectra were calibrated by setting the signal corresponding to Si—C or Si(IV)—O in the Si 2p level at 100.6 eV or 103.5 eV, depending on the sample, in accordance to literature [29]. For comparison, the spectra were normalized to the same area. For some samples, deconvolution of the Pt 4f spectra was carried out to evaluate the contributions of the individual oxidation states. Peaks were adjusted using CASA XPS software® under the following constraints: peak positions, half width at full maxima (FWHM), distance (3.3 eV) and relative area ratios (4/3) of the 4f_{7/2}–4f_{5/2} doublet, according to literature [16,30]. The Pt 4 f_{7/2} peak positions were set as follows: metallic Pt: 70–71 eV, Pt^{II}: 72–72.3 eV and Pt^{IV}: 73.8–74 eV and the FWHM were set with ±0.2 eV at Pt: 1.2 eV, Pt^{II}: 1.7 eV and Pt^{IV}: 1.9 eV [16,30,31]. The area of the individual peaks signified the amount of Pt in different oxidation states. Monte Carlo error analysis was performed for error estimates also using CASA XPS software®.

2.4. Catalytic tests

Catalytic tests were performed in a fixed bed quartz reactor (20 mm diameter, 500 mm length). The activity of the empty reactor, the quartz wool and the bare supports was first tested and has shown around 30% conversion at 450 °C and 15% at 150 °C.

Prior to each experiment, the reactor was loaded with 10 mg of supported catalyst plus 90 mg of bare support (both catalyst and support previously mortar mixed) over quartz wool, to ensure covering the whole reactor section. The catalyst amount was first optimized to achieve a sigmoid conversion vs temperature curve. These conditions are essential to evaluate catalytic properties (activation energy, T₅₀, etc). Unless indicated the contrary, catalysts were tested with no previous conditioning treatment. The reactor was heated from outside using an electric furnace and temperature was controlled using a PID controller. Temperature was measured by a K-type thermocouple placed at the center of the packed bed.

Reactions were carried out with a feed mixture consisting of 200 ml min⁻¹ of 1% v/v mixture of H₂ in air. Such lean hydrogen mixture was selected for catalysts' comparison purposes as reported before [4]. Working gases (H₂ 99.999% and air) were measured through Bronkhorst® mass flow controllers and premixed in a chamber before feeding the reactor. High gas flow rate and low catalyst weight limits H₂ conversion and thus one can obtain the kinetics of the process controlled by the reaction at nearly isothermal conditions. A HP 5890 chromatograph was employed to measure H₂ amount, with a ShinCarbon® packed column and a

Table 1
Catalysts characteristics.

Catalyst	%Pt	Particle size (nm) TEM	No previous conditioning before test (oxidized form)				In-situ reduced before test		
			%Conversion at RT	T ₅₀ (°C)	Activity ^a at 50 °C (ml _{H2} min ⁻¹ g _{catalyst} ⁻¹)	bE _a (kJ mol ⁻¹)	T ₅₀ (°C)	Activity ^a at 50 °C (ml _{H2} min ⁻¹ g _{catalyst} ⁻¹)	bE _a (kJ mol ⁻¹)
0.5Pt/SiC	0.5	(5±4)	11	38	132	16	40	124	19
0.5Pt/SiCulfo	0.5	(7±5)	92	—	200	—	—	—	—
0.5Pt/SiO ₂	0.5	(1.5±0.8) many aggregates	9	50	101	20	28	164	33
0.5Pt/Al ₂ O ₃	0.5	(1.0±0.3)	0	>200	0	—	40	134	29
0.5Pt/TiO ₂	0.5	(0.9±0.2)	0	95	14.4	46	—	200	—

^a Extracted from the conversion vs temperature curve in cooling mode.

^b Apparent activation energy obtained from the Arrhenius plots as shown in Figs. 4S and 5S as Supporting information.

thermal conductivity detector. N₂ was used as the carrier gas. Catalytic tests were first done at RT and then the temperature was increased to 420 °C or 200 °C depending on the experiment. After the 420 °C were reached, the temperature was maintained during 1 h and then conversion vs temperature curve was measured during cooling down to RT. For those experiments heated to 200 °C, the conversion vs temperature curve was measured immediately during cooling down to RT.

Some catalytic experiments were conducted with previous reduction of the catalyst (*in situ*, 100 ml min⁻¹ N₂, 50 ml min⁻¹ H₂, 400 °C 4 h). After reduction, the reactor was cooled down under nitrogen to 250 °C and the catalysts were exposed to the 1% H₂/air mixture for some activation. The conversion vs temperature curve was measured from 200 °C to RT.

3. Results and discussion

3.1. Catalysts and supports

Fig. 1a shows XRD measurements performed on the 0.5 wt.% Pt catalysts over SiC, TiO₂, SiO₂ and Al₂O₃. For the 0.5Pt/SiC catalyst, broad diffraction peaks corresponding to the Pt metallic phase (ICDD 00-004-0802) were found. For the TiO₂, SiO₂ and Al₂O₃ supported catalysts, no diffraction peaks corresponding to metallic platinum or platinum oxide were found, indicating the presence of very small nanoparticles.

Fig. 2 shows the representative STEM/HAADF images of the 0.5 wt.% Pt catalysts over SiC, TiO₂, SiO₂ and Al₂O₃. Their corresponding histograms are also shown. The SiC supported catalyst shows medium size particles (5±4) nm while those TiO₂, SiO₂ and Al₂O₃ supported catalysts exhibit very small particles (around 1–2 nm, depending of the sample as shown in Table 1), in accordance to XRD measurements. The case of the 0.5Pt/SiO₂ sample is peculiar, because not only very small and disperse nanoparticles were obtained but also many big aggregates were found. The obtention of small and monodisperse particles for the TiO₂ and Al₂O₃ supports can be understood in terms of the interaction of the positively charged surface of the supports (Fig. 1S, supplied as Supporting info.) at the impregnation pH with the [PtCl₆]²⁻, [PtCl₅(H₂O)]⁻ species. These species were reported before as the most abundant in our impregnating conditions (pH and H₂PtCl₆ concentration) [32]. The medium size Pt particles for the SiC support and its broad size range can be understood by taking in account the presence of Si–C bonds on surface. The surface charge of the SiC is positive and relatively high at the impregnation pH as shown by zeta potential measurements, (Fig. 1S supplied as Supporting info.) probably due to the presence of surface acidic Si–O–C and Si–O–Si groups. However, XPS measurements on the Si 2p level (Fig. 2S, supplied as Supporting info.) show a high contribution of Si–C which explains that interactions of metal-complex anions

with the support are not well favored. In addition, the obtention of big aggregates for the SiO₂ supported sample is related to its low zeta potential at the impregnating pH (Fig. 1S).

With the idea of increasing the dispersion of the active phase on the SiC support, chemical treatment was employed in order to introduce hydrophilic surface Si–O groups. The SiC support was treated with a mixture of H₂SO₄ and HNO₃ during 1.5 h at 60 °C (SiC sulfo 1.5 h). Fig. 3S (supplied as Supporting information) shows the XRD diffractogram of the as received SiC in comparison to the acid treated sample. The SiC shows diffraction peaks at 35.6, 41.3, 60, and 71.7 °(2θ) which correspond to the β-SiC (ICDD 00-029-1129). The acid treated SiC (SiC sulfo 1.5 h) does not show any contribution of SiO₂ in the XRD diffractogram and shows only a slight increase in the intensity of the Si–O–Si IR signal respect to the SiC (Fig. 3S). This shows that the acidic treatment has not been very successful in introducing many surface Si–O groups.

Nevertheless acid treated SiC supports were impregnated with 0.5 wt.% Pt and compared with the 1 and 0.5 wt.% Pt catalysts supported on powdery SiC as received. XRD measurements are shown in Fig. 1b For the catalysts supported on as received SiC and acidic treated SiC, the broad peak at 39.76 °(2θ) assigned to (111) plane of Pt is clearly observed although does not permit to calculate crystal size accurately.

STEM/HAADF images are shown in Fig. 3 for the 0.5 wt% Pt impregnated catalysts on the as received SiC in comparison to the acid modified SiC powder. Their corresponding histograms are shown. Particle size for the as received SiC supported catalyst is medium and polydisperse (average size 5±4) nm as discussed above. The 0.5 Pt SiC sulfo sample also shows a polydisperse particle size distribution with an increase in the population of the small nanoparticles (0–2 nm) and also in the big nanoparticles (>10 nm) respect to the as received SiC supported catalyst, being the average particle size in the range 7±5 nm (see Table 1). What is clear from these results is that in our conditions, HNO₃/H₂SO₄ treatment was unsuccessful in the obtention of small and monodisperse Pt particle size as expected. Instead of that, a broad particle size population was obtained, including bigger particles. Similar result was reported for a Co/SiO₂ catalyst for the Fischer Tropsh reaction in which SiO₂ was treated with HNO₃ before impregnation and thus bigger Co particles were obtained [33].

Surface states were studied by XPS (Pt 4f level) for the prepared catalysts and results are shown in Fig. 4 (normalized for comparison). In the case of alumina supported catalyst there is a superimposition with the Al 2p level which makes the analysis of surface oxidation states of Pt very difficult. Deconvolution was carried out to differentiate surface oxidation states and the results are also shown in Fig. 4. The 0.5Pt/SiC sample has shown a poor signal which did not allow to obtain reliable deconvolution. Pt impregnated catalyst supported on titania does not show contribution of Pt⁰ (70–71 eV) but shows (60±1)% of Pt^{II} contri-

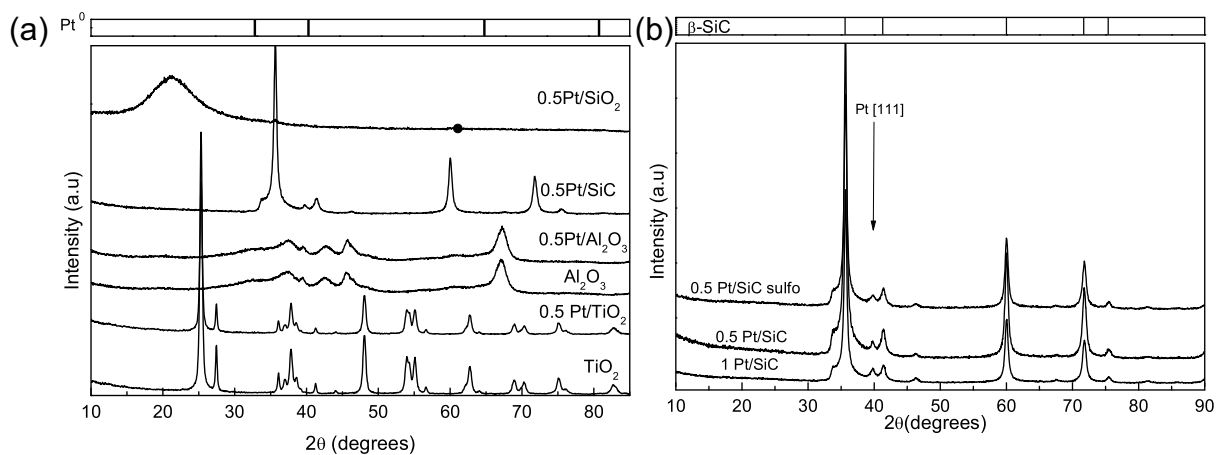


Fig. 1. XRD measurements performed on: (a) The 0.5Pt/SiC sample in comparison to the alumina, titania and silica supported catalysts. Bare TiO₂ and Al₂O₃ supports are also shown. Main peaks positions for reference metallic Pt are indicated (top bar diagram). (b) The 0.5Pt/SiC and 1Pt/SiC samples in comparison to the 0.5 wt% catalysts supported on previously acid modified SiC. Main peaks positions from reference β-SiC are also indicated at top bar diagram.

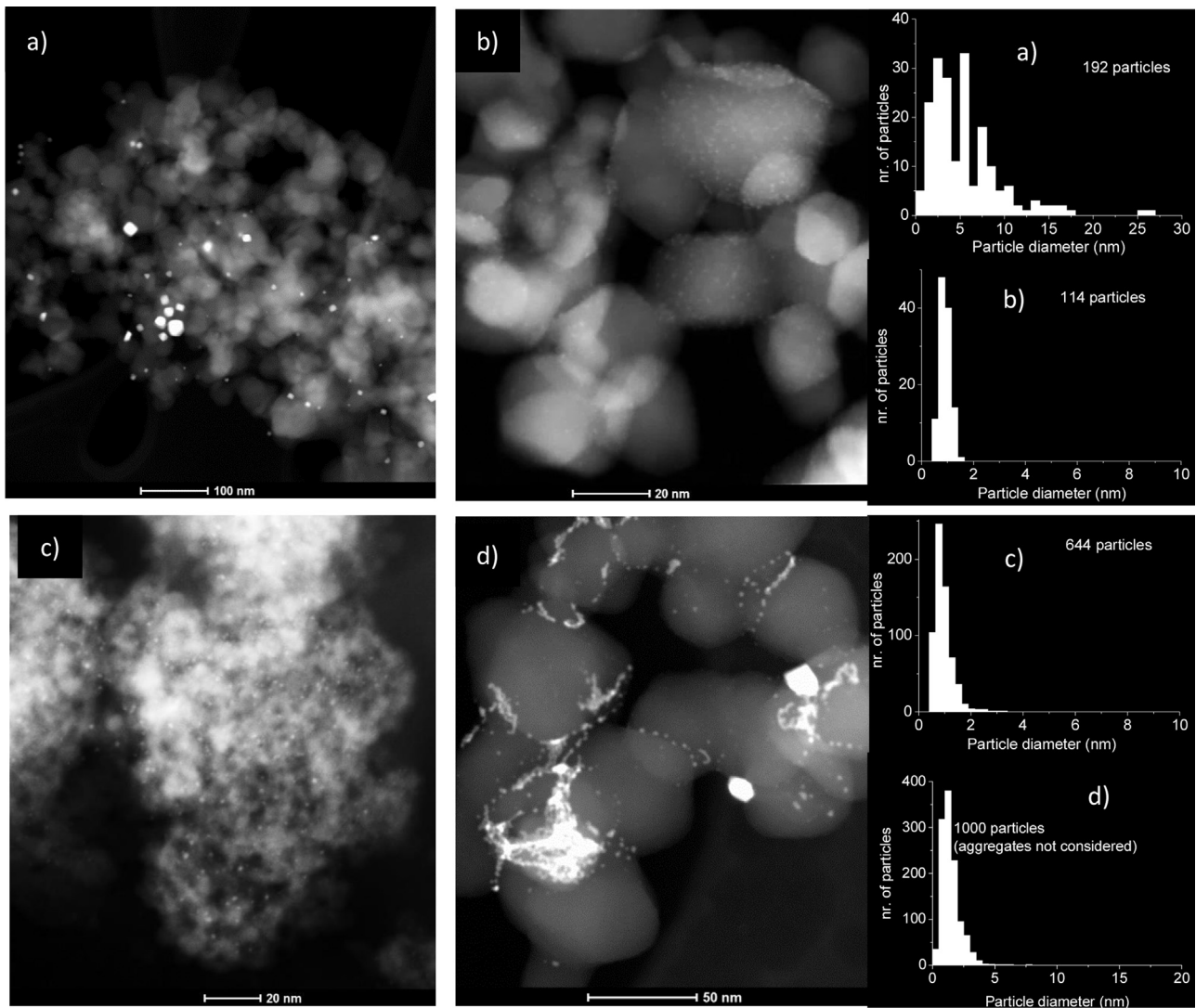


Fig. 2. Representative STEM/HAADF images of the 0.5 wt% Pt catalysts supported on (a) SiC, (b) TiO₂ (c) Al₂O₃ and (d) SiO₂ powders. The corresponding particle size histograms are also shown on the right.

bution and $(40 \pm 1)\%$ of Pt^{IV}. This high degree of surface oxidation is clearly consistent with the tiny particle size (less than 1 nm).

For the SiC supported Pt particles, an important contribution of metallic platinum can be qualitatively appreciated from the plot.

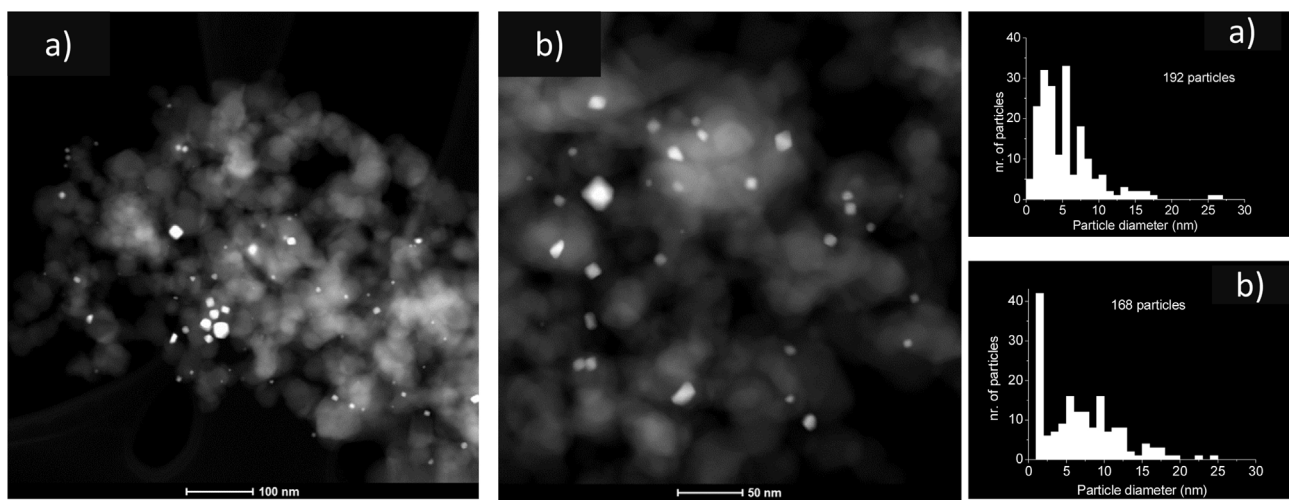


Fig. 3. Representative STEM/HAADF images of the Pt catalysts on commercial and modified SiC samples: (a) 0.5Pt/SiC (b) 0.5Pt/SiC sulfo. The corresponding particle size distribution plots are shown on the right.

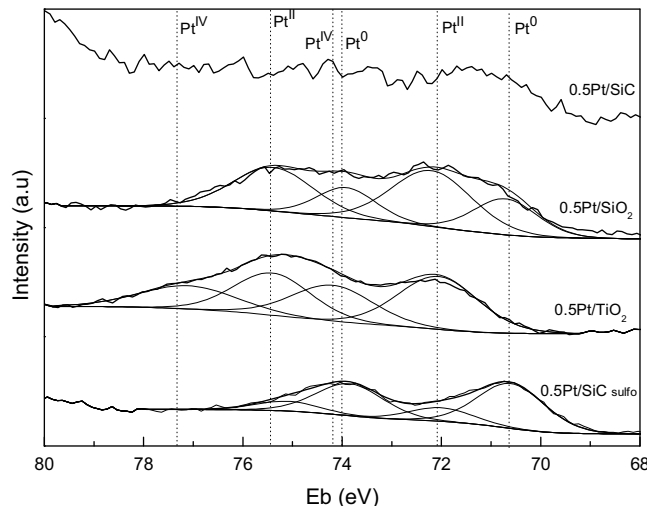


Fig. 4. XPS measurements on the Pt 4f level of the 0.5Pt/SiC sample in comparison to the titania, silica and acid treated SiC supported catalysts.

This is consistent with the medium particle size obtained during impregnation. In the case of the 0.5Pt/SiO₂ sample there is also some contribution of Pt⁰ ($34 \pm 2\%$) and the rest corresponds to Pt^{II} ($66 \pm 3\%$) in accordance to average particle size and the presence of aggregates.

Pt impregnated catalyst over acid treated SiC support was also studied by XPS (Fig. 4). Observation of the plot permits to conclude that the 0.5Pt/SiC sulfo sample shows the highest contribution of reduced Pt. The contribution of Pt⁰ is ($78 \pm 3\%$) of total while the remaining ($22 \pm 1\%$) corresponds to Pt^{II}. This result is connected to particle size, since this sample, has shown a high contribution of Pt particles of more than 5 nm size.

3.2. Catalytic activity

With the idea of a practical application and also considering that metal oxides are active for CHC, catalysts were tested in their oxidized (or partially oxidized) form unless indicated the contrary.

3.2.1. Effect of catalyst loading

The characterization of catalysts described above refers to the 0.5 wt% for all the investigated supports. In fact in first experiments

catalystsí loading was optimized. 1 wt.% Pt impregnated catalysts over SiC and over TiO₂ were tested first at RT (25°C) and 100% conversion was obtained for both materials. The temperature increased up to 40°C indicating that the heat released by the reaction was too high. For this reason catalyst loading was reduced to 0.5 wt% Pt and then 11% conversion for the SiC supported catalyst was measured while the conversion for the TiO₂ supported was 0% (Table 1). Nearly isothermal conditions were achieved for this 0.5 wt% Pt loading and were selected for further experiments.

3.2.2. Effect of catalystsí history. Reproducibility of the results

Many reports indicate that H₂/O₂ reaction mixtures strongly modify platinumís surface and causes irreproducible activity results [34–36]. For a Pt wire a high activity catalyst surface was found when temperature was decreased from 180°C ($E_a = 10 \text{ kJ mol}^{-1}$) while a less active surface was produced after the catalyst was raised from a low to a high temperature ($E_a = 35 \text{ kJ mol}^{-1}$). For this reason, 0.5 wt.% Pt impregnated catalysts on TiO₂ and SiC were tested in cooling mode under different initial conditions. First of all activity was measured at RT. Then, catalysts were heated to 200°C and immediately cooled down. On another (independent) experiment catalysts were heated to 420°C during one hour and then cooled down. In both cases, heating was performed under the 1% H₂/air atmosphere. Results are shown in Fig. 5. For both materials activity appears to increase with the heating temperature. For the 0.5 Pt/SiC catalyst (Fig. 5) a decrease in T₅₀ can be estimated in 9°C (T₅₀ not achieved for the 420°C heated catalyst) when the heating temperature was increased from 200 to 420°C . Fig. 5 also shows the conversion vs temperature curves for the 0.5% Pt/TiO₂ material where a decrease in T₅₀ of around 20°C was obtained when the initial temperature was 420°C respect to 200°C . Results obtained on TiO₂ and SiC supported catalysts indicates a clear sensitivity to the catalystsí history and an activation upon exposing to higher temperatures under the reaction (oxidizing) environment. This sensitivity to the heating history seems to be more pronounced for the TiO₂ supported than for the SiC supported Pt particles and can be ascribed to the formation of an active layer of strongly adsorbed oxygen species [34–36].

Regarding the reproducibility of results, working in excess of oxygen leads to more reproducible results than in stoichiometric conditions [35,36]. In particular, we found differences in T₅₀ of around $\pm 2^\circ\text{C}$ for the 0.5Pt/SiC sample and $\pm 4^\circ\text{C}$ for the 0.5Pt/TiO₂ sample in sets of two independent experiments. We consider that the reproducibility of our results in these conditions is acceptable.

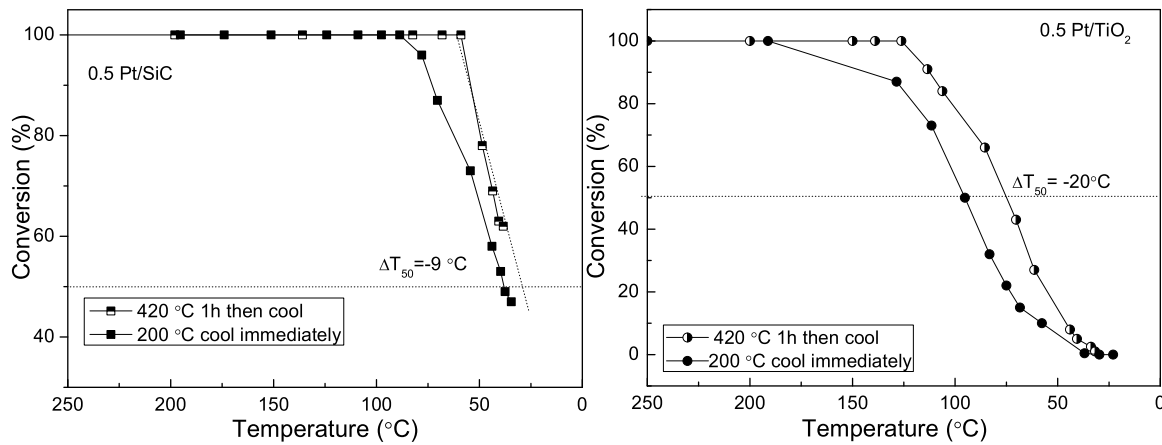


Fig. 5. Effect of catalysts' history. Comparison of the conversion vs temperature plots in cooling mode from 200 °C and 450 °C for the 0.5 Pt/SiC and the 0.5Pt/TiO₂ catalysts.

3.2.3. Comparison between different supports

The activity of the 0.5 wt% Pt impregnated catalysts over TiO₂, SiC, SiO₂ and Al₂O₃ was compared. First of all the conversion was measured at RT. Only the SiC and SiO₂ supported catalysts showed activity in these conditions (11 and 9% conversion respectively, according to Table 1). Conversion vs temperature curves were measured in cooling mode from 200 °C to RT for the four catalysts and results are shown in Fig. 6a. From the plot it is clear that the most active are the SiC and SiO₂ supported materials with a T₅₀ of around 38 and 50 °C respectively. The TiO₂ catalyst showed a medium activity with a T₅₀ equal to 95 °C. The alumina supported catalyst has shown no significant activity respect to the activity of the reactor, the glass wool and the support itself. Activities (expressed in mlH₂ min⁻¹ g_{catalyst}⁻¹) and apparent activation energies (obtained through the Arrhenius plot, shown in Fig. 4S) support the following activity trend: SiC supported ≥ SiO₂ supported > TiO₂ supported ≫ Al₂O₃ supported. As shown in Fig. 2 (particle size histograms) and Fig. 4 (XPS analyses) the activity of the SiC supported in comparison to the titania, silica and alumina supported catalysts in oxidized form can be correlated to particle size. Bigger particles, with a higher contribution of Pt⁰ are more active than those smaller and highly oxidized particles. The case of titania supported catalyst should be considered with special attention. Like the alumina supported counterpart, particle size is very small and around 1 nm. In both cases, the strength of the M–O bond is high enough to get completely oxidized particles. However, for Pt impregnated catalysts over TiO₂, activity is higher than over alumina. Previous reports have shown an enhancement in the activity of the TiO₂ supported catalysts owing to metal-support interactions which cannot be ruled out in our conditions [16]. Regarding the 0.5Pt/SiO₂ sample, there is a high contribution of big Pt aggregates whose effect in catalytic activity is difficult to evaluate. However, the high contribution of Pt⁰ in the XPS spectrum explains its higher activity respect to the titania and alumina supported particles.

For further insights on the CHC, catalysts were in-situ reduced before testing and then tested in 1% H₂/air mixture in cooling mode and results are shown in Fig. 6b and Table 1 (Arrhenius plots shown in Fig. 5S). The activity of the in-situ reduced 0.5Pt/SiC sample respect to the oxidized one remained unchanged. Apparent activation energies and activities (Table 1) did not significantly change with the pretreatment, indicating that catalysts' surface is similar to the fresh sample in both cases (partially oxidized). However, the titania and alumina supported catalysts increased significantly their activity. The 0.5Pt/SiO₂ sample, with both contribution of small particles and big aggregates has shown a medium increase in activity (T₅₀ = 28 °C vs 50 °C) probably due to the contribution of the small particles. These results support the idea of that the CHC

requires the presence of metallic sites for higher activity. Except for the titania supported catalyst, which probably combines the reduced state of Pt and oxygen vacancies to obtain the best activity, the activity seems not to be correlated to particle size. In this sense, Boudart et al. studied the activity of in-situ pre reduced Pt particles in a wide dispersion range (14–100%) and found that the CHC under excess of oxygen was structure insensitive. Corrosive chemisorption of oxygen could erase the surface anisotropies which exist on metal surfaces. However, our results obtained from previously in-situ reduced Pt particles are much more sensitive to catalysts' history than the ones obtained in oxidized form. A decrease in 33 °C in T₅₀ was found when the pre reduced 0.5Pt/Al₂O₃ catalyst was exposed to the 1% H₂/air reaction mixture at 250 °C instead of 200 °C (Fig. 6S, as Supporting information).

The interpretation of activity trends in CHC in this work is not straightforward because in our conditions for most catalysts the overall reaction mechanism follows a mixture of two mechanisms. A previous report explains that when CHC occurs in reductive reaction mixtures (when the ratio of H₂ to O₂ exceeds five) on a reduced Pt surface, H₂ is completely dissociated and competes with molecular oxygen for adsorption sites [36]. In completely oxidized surfaces and when the reaction mixtures are oxidant (when the ratio of O₂ to H₂ exceeds twenty), weakly adsorbed hydrogen species react with strongly adsorbed oxygen with no competition for adsorption sites [4,37]. In partially oxidized samples (which can be considered as a mixture of the two surfaces) under oxidant reaction mixtures, the overall mechanism is a mixture of the two. This mixture of mechanisms occurs in our samples with in-situ previous reduction as well as in the 0.5Pt/SiC and SiO₂ samples in oxidized form. For further comprehension of this, studies of catalysts after use and in operando should be performed but this exceeds the scope of the present work.

3.2.4. Activity of the Pt particles on previously acid treated SiC support

The catalyst supported on the previously acid treated SiC surface was investigated. The conversion of the 0.5 wt.% Pt catalyst over modified SiC was measured at RT and compared (Table 1). The highest activity was obtained for this catalyst (0.5 Pt/SiC sulfo, 92% conversion) followed by the 0.5 Pt/SiC material which has shown 11% conversion. This trend in activities was later confirmed with the conversion vs. temperature curves as shown in Fig. 7. The resulting trend is: 0.5 Pt/SiC sulfo ≫ 0.5 Pt/SiC. Those Pt particles supported on the sulfo treated SiC have shown the highest contribution of big particles according to Fig. 3 and correlates with the particle size effect explained in 3.2.3.

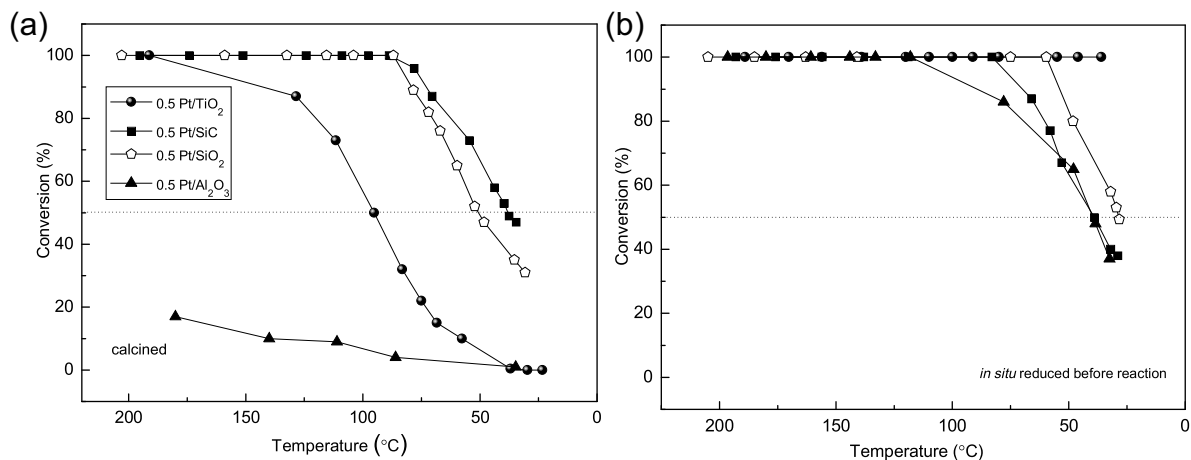


Fig. 6. Conversion vs temperature plot for the 0.5Pt/SiC sample in comparison to the alumina, titania and silica supported catalysts. (a) With no previous catalyst conditioning (oxidized or partially oxidized form) (b) With previous in-situ reduction before reaction.

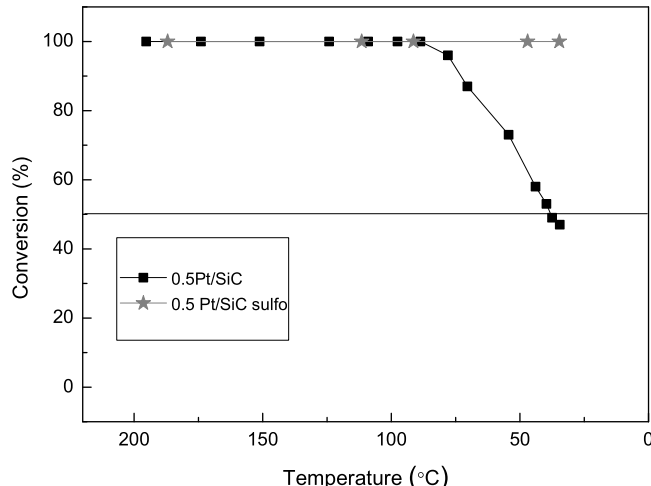


Fig. 7. Conversion vs temperature plots of the 0.5Pt/SiC sample in comparison to the Pt catalysts supported on previously acid modified SiC.

3.2.5. Comparison with literature

The comparison of catalysts with literature is difficult since it is hard to find papers in which materials were tested in exactly the same conditions as ours. Activity for CHC depends on catalysts' history, H₂ and O₂ concentration, total gas flowrate, amount of catalyst, nature and state of the metal (metal substituted more active than impregnated), type of support (reducible more active than inert), metal loading, etc [15,16,34–36].

Haruta and Sano screened metal oxides (300 mg) for CHC in air (1%H₂) and obtained a Volcano plot in which bulk PtO₂ has similar T₅₀ to our SiC supported catalyst [4]. From that plot it can also be derived that our TiO₂ supported catalyst has a T₅₀ similar to bulk Ag₂O [4]. Our SiC sulfo supported catalyst has similar activity to bulk PdO [4].

Madras et al. tested Pt and Pd substituted ceria based catalysts for CHC in air (3%H₂, 10 mg catalyst) and found that Ce_{0.98}Pd_{0.02}O_{2-δ} (Pd-substituted) and Pd/CeO₂ (Pd impregnated) had similar activity at 50 °C to our 0.5Pt/SiC sulfo in oxidized form and our 0.5Pt/TiO₂ with previous in-situ reduction (around 200 mlH₂ min⁻¹ g_{catalyst}⁻¹ all) [15]. However Ce_{0.83}Ti_{0.15}Pd_{0.02}O_{2-δ} and Ce_{0.83}Ti_{0.15}Pt_{0.02}O_{2-δ} catalysts showed higher activity at 50 °C than any of the catalysts presented herein (around 550 mlH₂ min⁻¹ g_{catalyst}⁻¹) [15].

In our previous work, we tested a commercial catalyst (0.27 wt% Pt/SiC-washcoat) which consisted of 2–20 nm Pt particles dispersed on alumina washcoat on monolithic SiC (mashed into granules) in similar conditions to herein. [18] We found a T₅₀ around 34 °C which is comparable to that obtained for our 0.5Pt/SiC (with higher Pt loading). However, activities show that the 0.27 wt% Pt/SiC-washcoat (38 mlH₂ min⁻¹ g_{catalyst}⁻¹) is less efficient than our 0.5Pt/SiC catalyst at 50 °C.

3.2.6. Durability upon cycling

Durability of the 0.5 wt% Pt catalysts over TiO₂ and SiC was tested upon cycling (5 cycles) and results are shown in Fig. 8. For both materials, the activity has shown an increase upon 5 cycles. However, the 0.5Pt/TiO₂ sample has shown a 20 °C decrease in T₅₀, while the 0.5Pt/SiC has shown a 10 °C decrease, indicating different sensitivity to the cycles. For a comprehension of this effect, both used samples were characterized by TEM and XPS. As described in the experimental section, for catalytic tests, samples are diluted 1/10 with bare support. This makes difficult the detection of Pt levels through XPS and also it is hard to find small particles by TEM for the used catalysts. Despite these difficulties, some data were obtained and results are shown in Fig. 9. Regarding the 0.5Pt/SiC sample, neither Pt 4f nor Pt 5d levels were detected by XPS. As we mentioned before due to lower dispersion the Pt signals were already difficult to detect before dilution. A series of STEM/HAADF images were studies and a representative one is depicted in Fig. 9a for the 0.5Pt/SiC sample together with its corresponding particle size distribution plot. The comparison of the particle size of the Pt particles after 5 cycles (5 ± 3) nm with the fresh catalyst (5 ± 4) nm shows no evidence of particle aggregation. Also, no evidence of aggregation or growth was found for the 0.5Pt/TiO₂ sample used in 5 cycles (Fig. 9b) respect to the initial fresh sample. In our conditions, particle aggregation seems not to be favored and does not explain the activation of both catalysts upon cycling.

XPS measurements on the Pt 4f level of the 0.5Pt/TiO₂ sample used 5 cycles in comparison to the fresh sample shows an increase in the contribution of Pt^{IV} (Fig. 9c). This result is connected with the results presented in Section 3.2.2, regarding catalyst's history. Exposure of catalysts to the reaction mixture produces an active oxide layer which activates catalysts. For the 0.5Pt/TiO₂ sample, the enhancement is higher because the reaction occurs by weak H₂ adsorption over strongly adsorbed oxygen, while for the 0.5Pt/SiC (partially oxidized) reaction occurs by a mixture of this mechanism and dissociative adsorption of H₂ and oxygen, as explained in Section 3.2.3. From a practical point of view, this finding is very

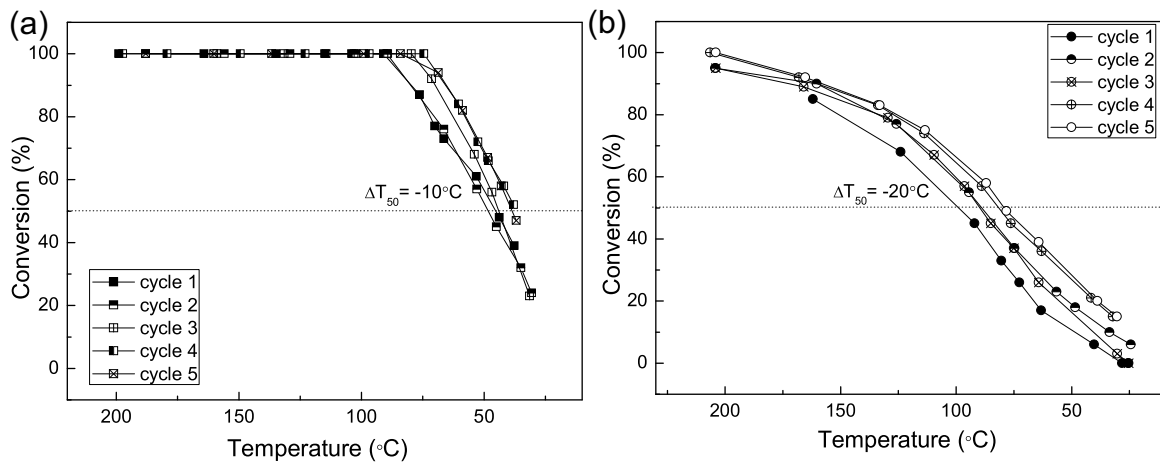


Fig. 8. Durability upon cycling (5 cycles) of (a) the 0.5Pt/SiC catalyst and (b) the 0.5Pt/TiO₂ sample.

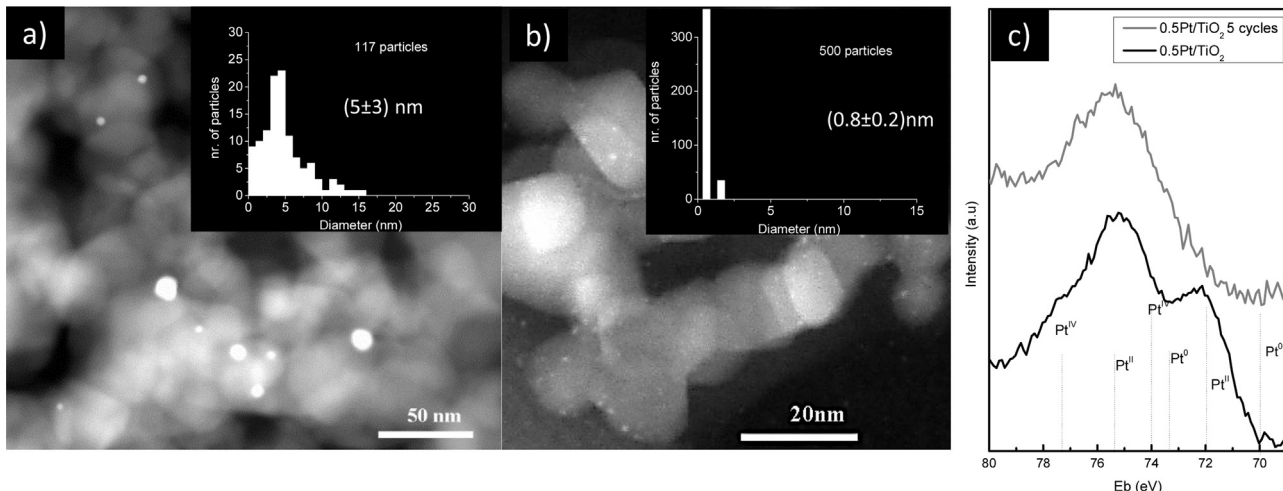


Fig. 9. Representative STEM/HAADF images of (a) the 0.5Pt/SiC and (b) the 0.5Pt/TiO₂ catalysts both after 5 cycles. The insets show the particle size distribution plot. (c) XPS measurements of the Pt 4f level on the fresh and used (5 cycles) 0.5Pt/TiO₂ sample.

interesting, since catalysts do not suffer from deactivation upon use. In practical applications in which the amounts of lean hydrogen mixtures are high, the heat generated by the reaction would increase the efficiency of the catalysts during operation.

4. Conclusions

In this work, Pt particles were prepared on commercial SiC (β -SiC) powder by pore volume impregnation with CPA and tested as catalysts for CHC under excess of oxygen. The activity was compared with those particles obtained impregnating CPA on traditional powdery supports such as titania, silica and alumina. Thinking of a practical application, catalysts were tested in their oxidized (or partially oxidized) form. The activity of the medium size Pt particles obtained on SiC was higher than those smaller obtained in other supports and increased upon exposure to the reaction mixture at high temperatures. No significant change in the activity of the SiC supported particles was found with previous in-situ pre-reduction of the catalyst. All these results point out that for practical applications in which lean hydrogen/air mixtures should be eliminated, the best activity is achieved with partially oxidized Pt surfaces as the ones obtained on SiC. Efforts to get high dispersion

on SiC seem to be unnecessary. Instead, the higher size Pt particles obtained with previous acid treatment on SiC have shown better activity. The catalyst was activated upon cycling when tested from 200 °C in cooling mode. For the design of a practical device, heating under the reaction mixture would be beneficial to the activity of the catalyst, and less dangerous than in-situ reducing in hydrogen atmosphere. However, if the desired application permitted in-situ reducing treatments, washcoating the SiC with TiO₂ would lead to the best activity probably because of the synergies between the amount of metallic Pt surface and the contribution of oxygen from the support.

Acknowledgements

Financial support is acknowledged from the Junta de Andalucía (grant PE2012-TEP862, EU co-financed by FEDER), the Spanish MINECO (grants CTQ2012-32519 and CTQ2015-65918-R, EU co-financed by FEDER) and the CSIC (PIE-201460E018). TEM measurements were performed at the Laboratory for Nanoscopies and Spectroscopies LANE at the ICMs. Authors thank Mrs. Inmaculada Rosa Cejudo for her very valuable technical support and to the reviewers for their valuable comments.

Appendix A. Supplementary data

Supplementary data associated with this article can be found, in the online version, at <http://dx.doi.org/10.1016/j.apcatb.2016.08.042>.

References

- [1] Andreas Züttel, Andreas Borgschulte, Louis Schlapbach, Hydrogen as a Future Energy Carrier, Wiley-VCH, 2008.
- [2] Louis Schlapbach, Andreas Züttel, *Nature* 414 (2001) 353–358.
- [3] John O’M. Bockris, *Int. J. Hydrogen Energy* 38 (2013) 2579–2588.
- [4] M. Haruta, H. Sano, *Int. J. Hydrogen Energy* 6 (1981) 601–608.
- [5] I. Wierza, A. Depiak, *Int. J. Hydrogen Energy* 29 (2004) 1303–1307.
- [6] M. Al-Garni, *Int. J. Hydrogen Energy* 22 (1997) 383–387.
- [7] W. Choi, S. Kwon, H.D. Shin, *Int. J. Hydrogen Energy* 33 (2008) 2400–2408.
- [8] a M. Haruta, Y. Souma, H. Sano, *Int. J. Hydrogen Energy* 7 (1982) 729–736;
b M. Haruta, H. Sano, *Int. J. Hydrogen Energy* 7 (1982) 737–740.
- [9] M. Haruta, H. Sano, *Int. J. Hydrogen Energy* 7 (1982) 801–807.
- [10] K. Ledjeff, M. Haruta, H. Sano, *Int. J. Hydrogen Energy* 12 (1986) 361–367.
- [11] F. Morfin, J.-C. Sabroux, A. Renouprez, *Appl. Catal. B: Environ.* 47 (2004) 47–58.
- [12] K.K. Sanap, S. Varma, S.B. Waghmode, S.R. Bharadwaj, *Int. J. Hydrogen Energy* 39 (2014) 15142–15155.
- [13] N. Meynet, A. Bentaïb, V. Giovangigli, *Combust. Flame* 161 (2014) 2192–2202.
- [14] C. Zhang, J. Zhang, J. Ma, *Int. J. Hydrogen Energy* 37 (2012) 12941–12946.
- [15] P.A. Deshpande, G. Madras, *Appl. Catal. B: Environ.* 100 (2010) 481–490.
- [16] P.A. Deshpande, G. Madras, *Phys. Chem. Chem. Phys.* 13 (2011) 708–718.
- [17] V.M. Shinde, G. Madras, *Catal. Today* 198 (2012) 270–279.
- [18] A. Fernández, G.M. Arzac, U.F. Vogt, F. Hosoglu, A. Borgschulte, M.C. Jiménez de Haro, O. Montes, A. Züttel, *Appl. Catal. B: Environ.* 180 (2016) 336–343.
- [19] R. Dhiman, E. Johnson, E.M. Skou, P. Morgen, S.M. Andersen, *J. Mater. Chem. A* 1 (2013) 6030–6036.
- [20] P. Marín, S. Ordóñez, F.V. Diez, *J. Chem. Technol. Biotechnol.* 87 (2012) 360–367.
- [21] I. Florea, M. Houllé, O. Ersen, L. Roiban, A. Deneuve, I. Janowska, P. Nguyen, C. Pham, C. Pham-Huu, *J. Phys. Chem. C* 113 (2009) 17711–17719.
- [22] P. Nguyen, C. Pham, *Appl. Catal. A* 391 (2011) 443–454.
- [23] M.J. Ledoux, C. Crouzet, C. Pham-Huu, V. Turines, K.D. Kourtakis, P.L. Mills, J.J. Lerou, *J. Catal.* 203 (2001) 495–508.
- [24] P. Nguyen, D. Edouard, J.M. Nhut, M.J. Ledoux, C. Pham-Huu, *Appl. Catal. B: Environ.* 76 (2007) 300–310.
- [25] S. Ivanova, E. Vanhaecke, B. Louis, S. Libs, M.J. Ledoux, S. Rigolet, C. Marichal, C. Pham, F. Luck, C. Pham-Huu, *ChemSusChem* 1 (2008) 851–857.
- [26] L. Yu, X. Liu, Y. Fang, C. Wang, Y. Sun, *Fuel* 112 (2013) 483–488.
- [27] Y. Liu, B. de Tymowski, F. Vigneron, I. Florea, O. Ersen, C. Meny, P. Nguyen, C. Pham, F. Luck, C. Pham-Huu, *ACS Catal.* 3 (2013) 393–404.
- [28] M. Boutonnet Kizling, P. Stenius, *Appl. Catal. B: Environ.* 1 (1992) 149–168.
- [29] D.J. Park, Y.I. Jung, H.G. Kim, J.Y. Park, Y.H. Koo, *Corros. Sci.* 88 (2014) 416–422.
- [30] D. Briggs, M.P. Seah, Practical Surface Analysis by Auger and X-ray Photoelectron Spectroscopy, John Wiley & Sons Ltd, 1983, ISBN 10: 047126279X.
- [31] L.K. Ono, J.R. Croy, H. Heinrich, B.R. Cuenya, *J. Phys. Chem. C* 115 (2011) 16856–16866.
- [32] B. Shelimov, J.F. Lambert, Michel Che, B. Didillon, *J. Am. Chem. Soc.* 121 (1999) 545–556.
- [33] Y. Zhang, Y. Liu, G. Yang, Y. Endo, N. Tsubaki, *Catal. Today* 142 (2009) 85–89.
- [34] F.V. Hanson, M. Boudart, *J. Catal.* 53 (1978) 56–67.
- [35] G.J.K. Acres, *Platin. Met. Rev.* 10 (1966) 60–64.
- [36] S.J. Gentry, J.G. Firth, A. Jones, *J. Chem. Soc. Faraday Trans. 1* (70) (1974) 600–604.